Fluctuation Contribution to the Far-Infrared Transmission of Lead Films*

D. B. Tanner†
Laboratory of Atomic and Solid State Physics, Cornell University, Ithaca, New York 14850
(Received 16 November 1972)

The transmission in the far infrared (2–40 cm^{-1}) of dirty very-thin lead films has been measured in the vicinity of the transition temperature T_c. The films were evaporated onto quartz substrates at or below 40 °K and were not warmed above this temperature between the evaporation and the transmission measurements. The resistances of the films were monitored simultaneously with the far-infrared measurements. The transmission of the films is reduced at the lowest frequencies (below 5 cm^{-1}) corresponding to an increase in the ac conductivity. The results are well described by theoretical conductivities which give a characteristic frequency of the fluctuations $\omega_F = (16k_BT/\pi\hbar)\,|T - T_c|/T_c$ both above and below T_c.

I. INTRODUCTION

This paper is a discussion of the far-infrared transmission of thin films of lead or lead-bismuth near the superconducting transition temperature. It is in this temperature interval that the effects of fluctuations in the superconducting order parameter are expected to give the biggest contribution to the film conductivity. It is in the far-infrared-frequency region that the effects of the lifetimes of the fluctuations are seen.

The dc resistive transitions of thin films have been extensively studied[1–7] since the original paper by Glover.[1] Even before this, Aslamazov and Larkin[8] published the first of a pair of papers in which they calculated the conductivity due to fluctuations using the microscopic theory and obtained the now famous result

$$\sigma' = e^2T_c/16\hbar d(T - T_c), \tag{1}$$

where d is the film thickness, T is the temperature, T_c is the transition temperature, and σ' is the extra conductivity due to the fluctuations. The measured conductivity is $\sigma = \sigma' + \sigma_N$, where σ_N is the normal-state conductivity. This result depends only on the thickness of the film and not on any other parameters. The constant τ_0 is

$$\tau_0 = e^2/16\hbar = 1.5\times10^{-5}\,\Omega^{-1}. \tag{2}$$

Measurements of the transition of lead films were made by Smith, Serin, and Abrahams[5] who found the Aslamazov-Larkin result; by Testardi *et al.*[6] who found the transitions in most samples to be narrower than Aslamazov-Larkin by about a factor of 2; and by Thompson *et al.*[7] who find the transition to be much narrower than Aslamazov-Larkin.

The conductivity above the transition temperature was derived using the time-dependent Ginsburg-Landau equation at essentially the same time by both Schmid[9] and Schmidt.[10] Schmid obtained the dc conductivity in the same form as Aslamazov and Larkin, Eq. (1). Schmidt also got this result for the dc conductivity and he further found the frequency dependence of the fluctuation conductivity. He has later calculated the conductivity as a function of frequency below the transition temperature.[11] The important parameter in both cases is the characteristic frequency given by

$$\omega_F = (16k_BT/\pi\hbar)\,|T - T_c|/T_c, \tag{3}$$

where k_B is Boltzman's constant. The fluctuation components of the conductivity have similar (but not exactly the same) forms both above and below T_c. It should be pointed out that the regular conductivity (that not involving fluctuations) is quite different in the two regimes. The normal-state conductivity has a real part equal to the dc conductivity and an imaginary part equal to zero. The superconducting-state conductivity can be found in the tables published by Miller.[12] These were derived from the theory of Mattis and Bardeen[13] and give the conductivities, σ_1^{MB}/σ_N and σ_2^{MB}/σ_N, as a function of frequency.

A calculation[14] using the time-dependent Ginsburg-Landau theory which is similar to that by Schmidt, but carried to higher frequencies, gives the following expressions for the conductivities. The total conductivities for $T > T_c$ are the following:

the real part

$$\frac{\sigma_1}{\sigma_N} = 1 + \tau_0 R_N^{\square}\left(\frac{T_c}{T - T_c}\right)\frac{k_BT}{\hbar\omega}\,(1 - e^{-\hbar\omega/k_BT})\,\frac{\omega_F}{\omega}\left(\pi - 2\tan^{-1}\frac{\omega_F}{\omega} - \frac{\omega_F}{\omega}\ln(1 + \omega^2/\omega_F^2)\right); \tag{4}$$

the imaginary part

$$\frac{\sigma_2}{\sigma_N}=\tau_0 R_N^{\square}\left(\frac{T_c}{T-T_c}\right)\frac{k_BT}{\hbar\omega}\left(1-e^{-\hbar\omega/k_BT}\right)\frac{\omega_F}{\omega}\left(-2+\pi\frac{\omega_F}{\omega}-2\frac{\omega_F}{\omega}\tan^{-1}\frac{\omega_F}{\omega}+\ln(1+\omega^2/\omega_F^2)\right). \quad (5)$$

For $T<T_c$ they are the following:

the real part

$$\frac{\sigma_1}{\sigma_N}=\frac{\sigma_1^{MB}}{\sigma_N}+\tau_0 R_N^{\square}\left(\frac{T_c}{T_c-T}\right)\frac{k_BT}{\hbar\omega}\left(1-e^{-\hbar\omega/k_BT}\right)\frac{\omega/\omega_F}{1+\omega^2/\omega_F^2}\left(\pi-2\tan^{-1}\left(\frac{\omega_F}{\omega}\right)-\frac{\omega_F}{\omega}\ln[\tfrac{1}{4}(1+\omega^2/\omega_F^2)]\right); \quad (6)$$

the imaginary part

$$\frac{\sigma_2}{\sigma_N}=\frac{\sigma_2^{MB}}{\sigma_N}+\tau_0 R_N^{\square}\left(\frac{T_c}{T_c-T}\right)\frac{k_BT}{\hbar\omega}\left(1-e^{-\hbar\omega/k_BT}\right)\frac{1}{1+\omega^2/\omega_F^2}\left(\pi-2\tan^{-1}\frac{\omega_F}{\omega}+\frac{\omega}{\omega_F}\ln[\tfrac{1}{4}(1+\omega^2/\omega_F^2)]\right). \quad (7)$$

In these expressions, $R_N^{\square}$ is the resistance the film would have if it were square. For frequencies low enough that

$$(k_BT/\hbar\omega)(1-e^{-\hbar\omega/k_BT})=1,$$

they reduce to those published by Schmidt.

The theory has been extended to the clean limit by Eilenberger[15] where momentum conservation requires that the complex conductivity in the normal state be multiplied by a factor $(1+i\omega\tau)^{-2}$. τ is the relaxation time of the normal electrons.

These expressions for the conductivity can be used to calculate the transmission of a film, as discussed by Hadley and Dennison.[16] For the case of a very-thin film, the reflection and transmission of the film can be found very easily from the boundary conditions on the field vectors by treating the film as a surface sheet of current, having current per unit area $K=jd=\sigma Ed$, where E is the (continuous) electric field vector on each side of the film. Internal reflections within the substrate must also be considered. For a thick substrate or a substrate with nonparallel sides, the intensity transmission ratio is

$$\mathcal{T}=\mathcal{T}_1\mathcal{T}_2/(1-\mathcal{R}_1\mathcal{R}_2), \quad (8)$$

where the transmission and reflection of the film (the first surface coefficients) are

$$\mathcal{T}_1=\frac{4n}{(n+1+Z_0\sigma_1 d)^2+(Z_0\sigma_2 d)^2}, \quad (9)$$

$$\mathcal{R}_1=\frac{(n-1+Z_0\sigma_1 d)^2+(Z_0\sigma_2 d)^2}{(n+1+Z_0\sigma_1 d)^2+(Z_0\sigma_2 d)^2}. \quad (10)$$

The transmission and reflection of the second surface are

$$\mathcal{T}_2=4n/(n+1)^2, \quad (11)$$

$$\mathcal{R}_2=[(n-1)/(n+1)]^2, \quad (12)$$

where n is the index of refraction of the substrate and Z_0 is the impedance of free space (377 Ω in practical units).

There have been measurements of the fluctuation conductivity at microwave frequencies by two groups. D' Aiello and Freedman[17] measured the transmission of aluminum films both above and below T_c at 20 GHz (0.67 cm^{-1}) and found no extra conductivity. Their results did not agree with the Schmidt theory. Lehoczky and Briscoe[18] measured the transmission and reflection of lead films both above and below the transition at three frequencies (0.7, 1.2, and 2.3 cm^{-1}) and found excellent agreement with Schmidt's theory.

II. EXPERIMENTAL TECHNIQUES

These measurements were made using Fourier-transform spectroscopic techniques. The interferometer was the lamellar grating described by Nolt, Kirby, Lytle, and Sievers.[19] The detector was a bolometer operating at pumped-^{3}He temperatures similar to that described by Drew and Sievers.[20] The output of the detector was connected through an appropriate series of amplifiers on line to a PDP-11 computer. This computer gave a real-time analysis and display of the spectral data as the run progressed, using a program written and described by Kahan.[21]

The cryostat used in these measurements is shown schematically in Fig. 1. It contains the evaporator used for making the films, the detector, and a charcoal pump. The evaporator is constructed as an insert which may be removed from the main system to allow the use of other sample inserts. The ^{3}He refrigerator in the main part is a sealed system and contains no moving parts. At the beginning of a run liquid ^{4}He was transferred into an outer glass Dewar (not shown) which surrounds the cryostat, then the inner ^{4}He container was filled through a needle valve and pumped by an external mechanical pump to 1 °K. The charcoal pump remained warm, protected by vacuum isolation, so the ^{3}He gas in the system condensed and dripped down into the ^{3}He pot. After 20 min or so when the ^{3}He had all condensed, He exchange gas was admitted to the vacuum can surrounding the charcoal pump. This cooled rapidly to 4.2 °K and equally rapidly pumped the ^{3}He to near 0.31 °K. The three STP liters of ^{3}He gas used gave an oper-

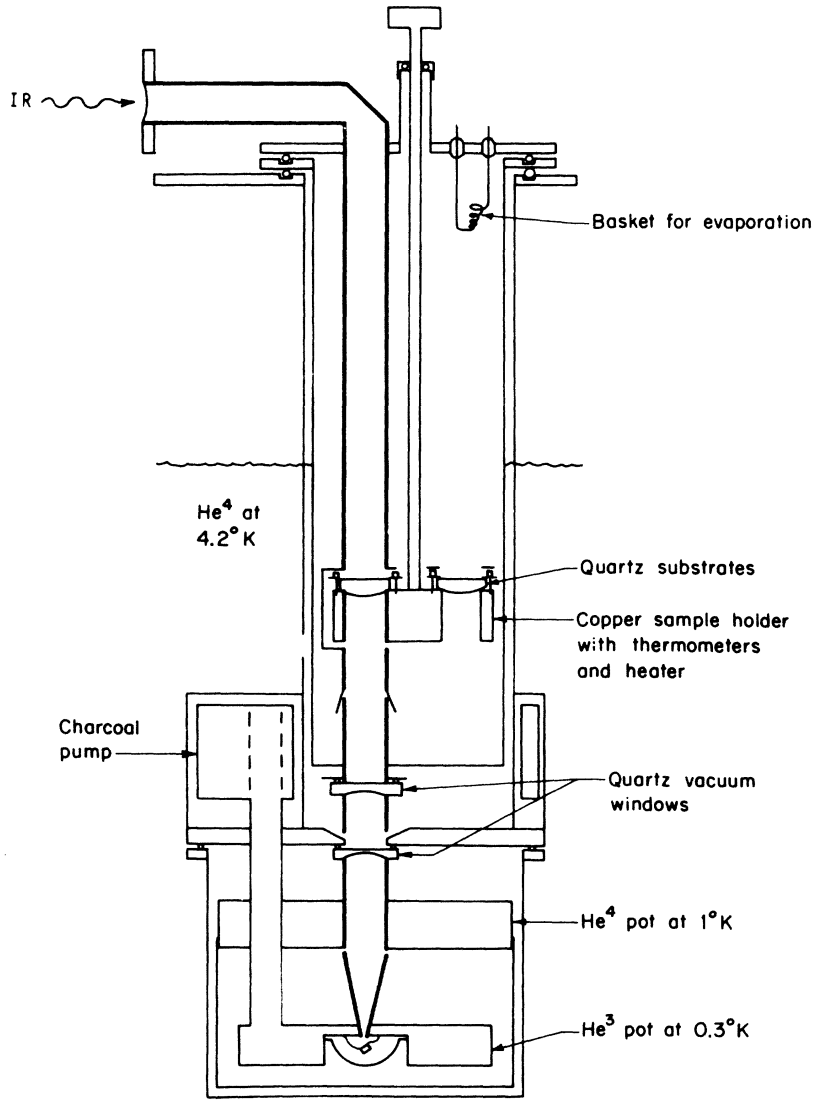

FIG. 1. Sketch of detector cryostat and evaporator insert. Glass liquid-helium and liquid-nitrogen Dewars surround the cryostat.

ating time of 36 h at this temperature.

The evaporator insert is a long stainless-steel tube with a quartz vacuum window at the bottom. The top plate carries the spiral-wound tungsten basket from which the evaporation takes place. The polished quartz substrates are held by brass clamps to the copper sample rotator using indium pads for good thermal contact. The sample holder has two positions. In one the substrate is in place for evaporation and after the evaporation a rotation of 180° brings the film into the far-infrared beam and puts the other substrate in position for evaporation.

Attached to the sample rotator are a carbon resistor and a heater for the Artronix temperature controller and another carbon resistor for a resistance bridge. There are four leads connected to each film in order to allow the film resistance to be measured using a four-probe technique. These leads are attached with indium solder to four narrow gold strips that had been evaporated onto the substrates before they were mounted. The copper sample holder is hollow and there exists the capability of transferring liquid helium into it through the hollow rotator rod, but this has not proven to work very well.

After the detector was operating and the outer liquid-helium container filled, the evaporation was done. At this time the pressure in the evaporator, as measured by an ionization gauge at the top, was near 10^{-6} torr. The sample holder had cooled to around 40 °K. During the evaporation, the dc resistance of the film was monitored, mostly to determine when the film became electrically continuous. This was done by putting 60 μV in series with a 10 kΩ resistor across the leads to the film,

TABLE I. Various film parameters.

Film numbers	3	5	6	7
Deposition temperature (°K)	40	26	30	25
Evaporation time (min)	3	2	3	3
Evaporation pressure (torr)	9×10^{-7}	7×10^{-7}	7×10^{-7}	3×10^{-6}
dc square resistance, $R_N^{\square}$ (Ω)	5470	3010	910	1430
FIR sheet resistance, $R_N^{\square}$ (Ω)	1600	820	440	1100
FIR transmission, $\mathcal{T}_N$	0.88	0.76	0.61	0.81
Thickness, d (Å)	10	14	20	12
Transition temperature, T_c (°K)	6.423	6.914	6.844	6.660
Aslamazov-Larkin parameter, τ_0 (Ω^{-1})	0.98×10^{-5}	0.96×10^{-5}	0.89×10^{-5}	0.89×10^{-5}
Critical width, $\tau_0 R_N^{\square} T_c$ (°K)	0.100	0.054	0.026	0.064

and measuring the voltage across the film. As the film resistance decreased during deposition the voltage across it also decreased. With this arrangement it was always possible to get a continuous film and easy to get close to a desired resistance.

The evaporation rate was about 2 Å per min; it took 3 min to get a continuous lead film. After two films had been deposited sufficient helium exchange gas was added to the evaporator volume to bring the film temperature to 4.2 °K and the far-infrared and dc-resistance measurements began.

Two or three passes through the transition region were made to get the far-infrared-transmission data. The dc resistance was measured on the first pass and was monitored constantly while an interferogram was being taken. It was used to make manual fine adjustments to the temperature controller. The dc resistance is a very sensitive thermometer in the transition region. In this way, the drift during an interferogram could be held to ± 0.005 °K.

III. SAMPLE PARAMETERS

During these experiments, measurements were made on seven lead films and one blank substrate. The films have been numbered Pb 1 through Pb 7. For the first six films, the basket in the evaporator was charged with an alloy of lead (Cominco 99.999%) with a 4-at.% bismuth (Cominco 99.9999%). The purpose of the bismuth was to decrease the normal-state conductivity. This was felt to be unnecessary so Pb 7 was made from the pure lead alone.

Four of the films, Pb 3, Pb 5, Pb 6, and Pb 7, produced successful simultaneous measurements of far-infrared transmission in the fluctuation region, dc resistance, and temperature. The experiments on three of the films were unsuccessful for various reasons: The detector system was unacceptably noisy during the run on Pb 1 and Pb 2. In addition, Pb 2 was quite thick so that its transmission was very low. Pb 4, on the other hand, was too thin; it was almost perfectly transparent. Qualitative fluctuation effects were observed in both Pb 1 and Pb 4, but a detailed comparison with theory was not made.

Various parameters useful in discussing the remaining films are displayed in Table I. The temperature at which the films were deposited is shown in the first line. This is also the highest temperature to which the films were submitted until the end of the measurements and so indicates the state of annealing of the films. It was always less than 40 °K. The major anneal in an amorphous film should occur near the Debye temperature which in lead is 96 °K. There was a big change in resistance in these films between 80 and 100 °K. Most of them became discontinuous at these temperatures and all increased their resistance. Strongin *et al.*[22] have measured the resistance of several lead films on different substrates and find that some annealing begins even at 7 °K, the transition temperature, and continues as the temperature is increased. By evaporating the films at a higher temperature than ever reached during repeated passes through the transition region any problems due to changing residual resistance during the experiment were avoided. At the end of the infrared experiments the resistance was generally measured as the films were warmed up to nitrogen temperatures. The resistance would increase slightly, indicating that there was no major annealing going on.

The next two rows give the time that the evaporation took and the pressure at the beginning of the evaporation. This pressure was measured by the ionization gauge at the top of the evaporator.

The square or sheet resistance in the normal state is the major parameter of the films. It is given in the next two rows of the table. The dc square resistance is just

$$R_N^{\square}=\frac{1}{\sigma_N d}=R_N\frac{w}{L}, \tag{13}$$

where σ_N is the zero-frequency electrical conduc-

tivity of the film, R_N is the measured residual resistance, and d, L, and w are its thickness, length, and width, respectively. The conductivity and thickness are not easy to measure in independent ways for a thin sample but the square resistance can be gotten by multiplying the measured residual resistance by the ratio of width to length. Another and perhaps more reliable measure of the square resistance of very-thin films can come from comparing the infrared transmission of the films to that of a blank substrate. The formulas to use are Eqs. (8)–(12). The infrared measure of $R_N^{\square}$ is equal to the dc value when $\omega\tau \ll 1$, so that $\sigma_1 = \sigma_N$, $\sigma_2 = 0$. This is surely the case for these very-thin films. The far-infrared-transmission ratios from which the sheet resistances were calculated are shown in the next row.

Inspection of Table I shows that the far-infrared values for $R_N^{\square}$ are in some cases almost a factor of 4 smaller than the dc values, the deviations being the largest in the thinner films. It is likely that the infrared value is the more accurate. The geometry of the film was far from ideal for dc measurements; it was wider than it was long and had curved sides whose contribution to the conductivity is hard to estimate. Any decrease in the effective width of the film would lower its square resistance. Secondly, the far-infrared radiation tends to average over point imperfections in the film. The infrared radiation measures the average conductivity in an area approximately the wavelength squared. Because of this it is insensitive to small holes or cracks in the film. Similarly, it is insensitive to a few scratches in the substrate which, if across the film, would seriously affect the dc resistance.

The thickness can be estimated in two ways.[23] For a very-thin film one would expect the mean free path to be[24]

$$l = \tfrac{8}{3}d$$

assuming diffuse scattering at the surface. Then the square resistance is

$$R_N^{\square} = 3mv_F/8ne^2d^2,$$

from which d can be found.

A check on this can be obtained for those films that exhibit temperature dependence in the resistance between the lowest temperatures and liquid-nitrogen temperature. Then

$$R^{\square}(T) - R_N^{\square} = \rho(T)\,1/d,$$

where $\rho(T)$ is the bulk resistivity at the temperature T. When available, this gave thicknesses similar to the first method.

In Fig. 2 is plotted the resistivity ratio, R/R_N, of the films versus temperature. As can be seen, the resistive transition is broad; the films exhibit considerable extra conductivity; and there is something of a tail in the resistance below the transition. It is the presence of this tail (whether a real or bogus phenomenon) that makes determination of the transition temperature difficult. Not immediately evident from the figure, but true nonetheless, is that the transition is narrower by about 40% in all of these films than would be predicted by the Aslamazov-Larkin formula, Eq. (1). It is thus necessary to determine an empirical value for the constant τ_0 applicable to these films. This requires the extraction of two parameters (T_c and τ_0) from one set of data. This was done by adjusting both T_c and τ_0 until the resistance data above T_c all agreed with

$$R_N/R = \sigma/\sigma_N = 1 + \tau_0 R_N^{\square}[T_c/(T - T_c)]$$

using the far-infrared value for $R_N^{\square}$. The final value for T_c was between 1 and 30 m °K below an initial graphical estimate, not a major change. All of the films had values for τ_0 within 5% of the average 0.93×10^{-5}. The values for T_c and τ_0 are in the ninth and tenth rows of the table. Last is the critical width. This is $\Delta T = \tau_0 R_N^{\square} T_c$.

IV. FAR-INFRARED RESULTS

In the next several figures are presented the results of the far-infrared measurements. The vertical axis is the transmission ratio, $\mathcal{T}_F/\mathcal{T}_N$, and the horizontal axis is the frequency (in cm^{-1} along the bottom and Hz along the top). The experimental data are shown as points and the theo-

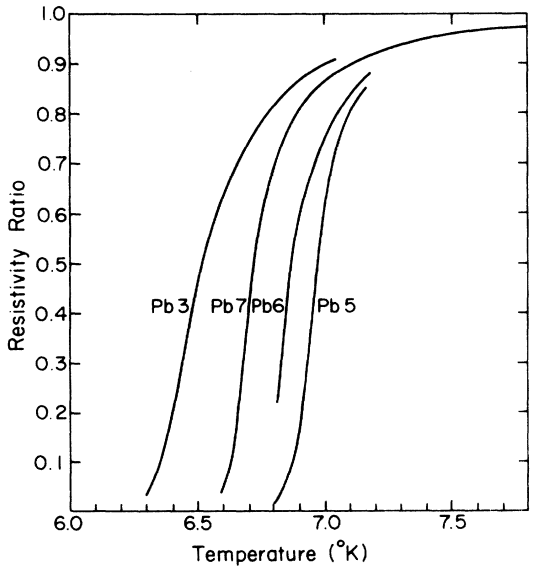

FIG. 2. Resistive transition of the films.

retical curves as solid lines. Now, the transmission curves have all been shifted vertically so as to separate them; the places where the experimental curves all cross 1 are indicated by the figures 1 on the left-hand side of the plots and also by the dashed horizontal line on each side of the data. On the left-hand side is a scale or ruler which shows the magnitude of the changes in the transmission ratio. Each division corresponds to a 1% change.

In all of the plots of $\mathcal{T}_F/\mathcal{T}_N$ vs frequency the theoretical curves have been slid upwards by a small amount in order to make them fit with the experimental points in the six to eight wave-number range. The theoretical curves are never larger than 1 for $T > T_c$ while the experimental curves all are at high frequencies. The amount of the required upward shift varies with temperature, being 0.6% at the high temperatures and 1.4% at the low temperatures.

There are error bars on representative points in all of the figures. These are calculated from the standard deviation of the spectrum and the value of the spectrum at the given frequency. Because of the low-pass filter used to give a high-frequency cutoff, the last few points of the spectrum are always nearly zero and their standard deviation can be computed to give a measure of the noise.

Figure 3 presents the results for Pb 3 as a function of frequency. Pb 3 was the thinnest film ($R_N = 1600\ \Omega$) and had data at the most temperatures. With the exception of the rigid vertical shift, there has been no fitting of the data. The values of τ_0 and T_c used are those from the dc-resistance measurements. The fit between the experimental points and the theoretical calculations is close to within the noise.

The four curves that extend to higher frequencies are the result of overlapping measurements with three different high-frequency limits or cutoffs, taking the average in the overlap region. The cutoffs were 50, 21, and 14 cm^{-1}. The numerical values of the transmission ratios differed by no more than 0.2% in the overlap region. The 21-cm^{-1} cutoff runs were used as a standard and the others were fitted to them. The curves that stop at the lower frequencies were measured only with the 21-cm^{-1} cutoff.

Figures 4, 5, and 6 show the transmission data for the other films, Pb 5, Pb 6, and Pb 7, respectively. In Pb 5 all of the runs were made at temperatures above the transition temperature and with an 18-cm^{-1} high-frequency cutoff. Pb 6 was the thickest film on which data were taken. All of the temperatures were above T_c again, although the error in the lowest-temperature run ($T - T_c = 0.001\ °K$) is 0.005 °K at least. It could be either above or below T_c. Both 18- and 66-cm^{-1} cutoff runs were made. Pb 7 was the only all-lead film. There was no bismuth in the evaporant. One of the interferograms was recorded for temperatures below T_c and both 16- and 40-cm^{-1} cutoffs were used.

V. DISCUSSION

If "best" is defined in terms of the fit between the experimental data and the theoretical points, then Pb 3 is the best film. It is followed closely by Pb 5 and Pb 6, with Pb 7 somewhat further back. With the exception of two measurements on Pb 7 and two on Pb 3, the deviations in fit are less than 0.5%. They are largest at the lowest frequencies (where the infrared source is the weakest) and at temperatures below T_c. Most of the deviations above T_c are due to varying signal-to-noise condition on different days.

Most of the discussion below is concerned with Pb 3 because it gave the best results and because data were taken at the most temperatures. Pb 5 or Pb 6 would have served almost as well for this, but Pb 7 is too noisy to bring out all of the finer points.

Figures 7 and 8 show the behavior of the conductivities above and below T_c for Pb 3. These

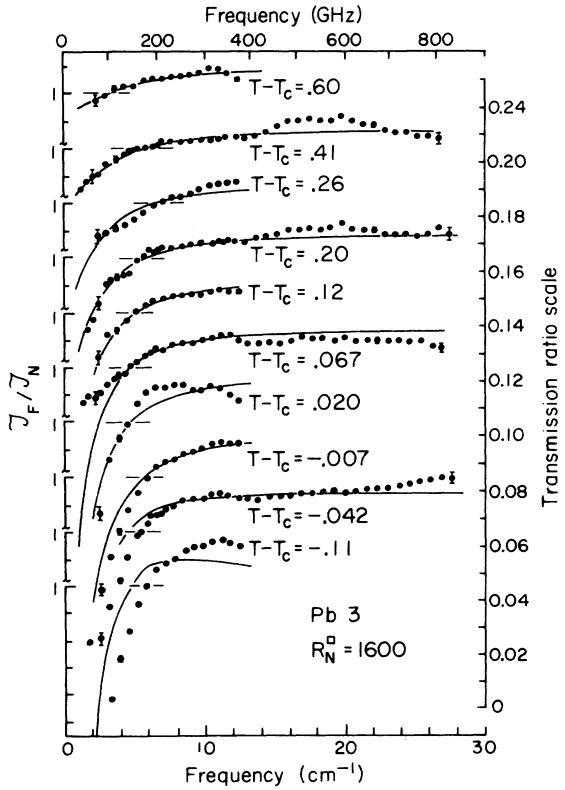

FIG. 3. Transmission ratio vs frequency for Pb 3.

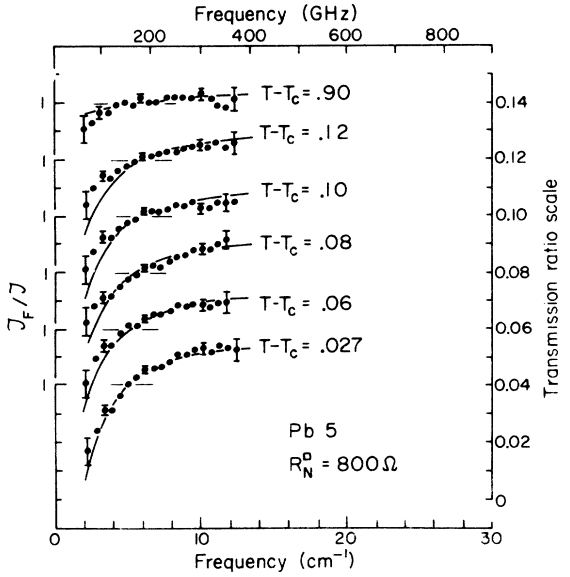

FIG. 4. Transmission ratio vs frequency for Pb 5.

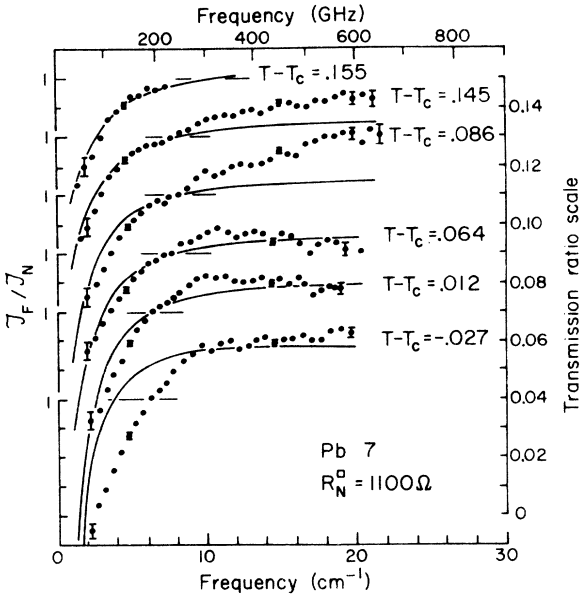

FIG. 6. Transmission ratio vs frequency for Pb 7.

are the total conductivities used to calculate the transmission ratios. The characteristic frequency ω_F is indicated by a cross mark on each of the curves.

Above the transition, the real part is a maximum at zero frequency, rolling off at the characteristic frequency ω_F to zero. The imaginary part is zero at zero frequency, rises to a peak near ω_F, and then drops to zero again. As the temperature gets closer to T_c, the heights of the maxima are increased and the characteristic frequency is reduced.

Below T_c the real part looks like the real part above T_c very near the transition and then goes over to the Mattis-Bardeen form as the temperature is decreased. There is little temperature dependence at low frequency. The imaginary part has the $1/\omega$ form with little temperature dependence near T_c, beginning to grow as the temperature falls.

The forms used here, both for temperature above and below the transition are the same as those obtained by Schmidt if the frequencies are restricted to low-enough values so that

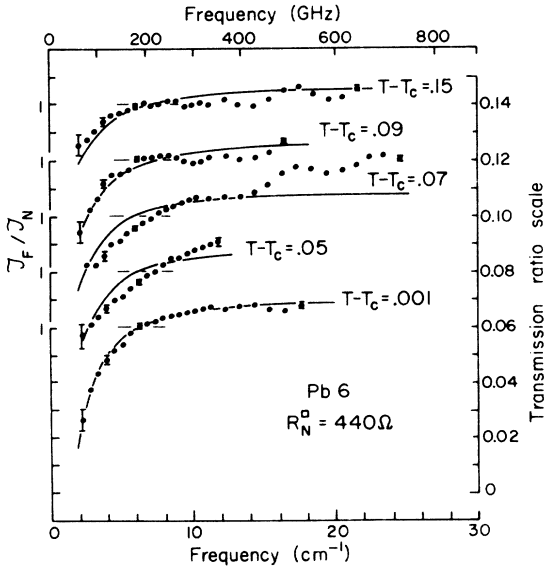

FIG. 5. Transmission ratio vs frequency for Pb 6.

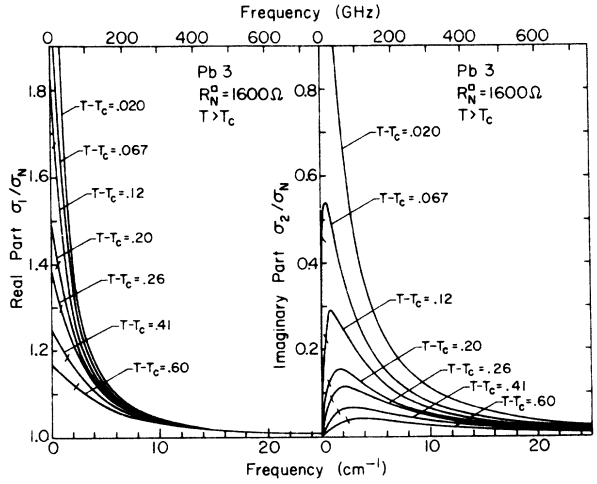

FIG. 7. Real and imaginary parts of the conductivity of a film above the transition temperature.

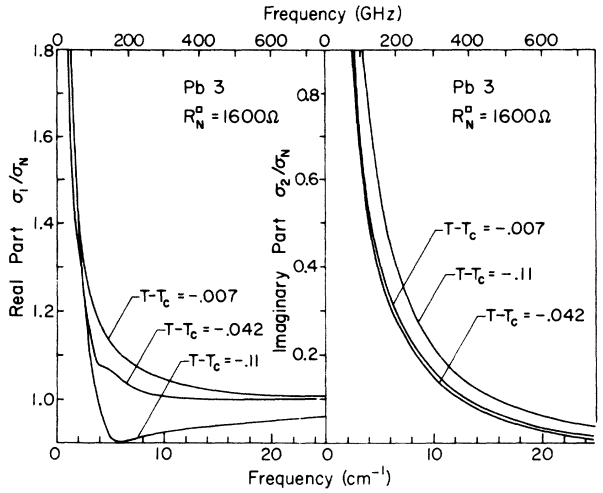

FIG. 8. Real and imaginary parts of the conductivity of a film below the transition temperature.

$$(k_B T/\hbar\omega)(1-e^{-\hbar\omega/k_B T}) = 1.$$

This factor forces the extra conductivities to fall off to zero faster at high frequencies (by a factor of $1/\omega$) than do Schmidt's results.

The only fitting of the theoretical curves to the experimental points was the upward shift of the theoretical curves. These are always less than 1 for $T > T_c$ while the experimental points always cross 1. There are two possibilities why this might occur: (i) The Ferrell-Glover sum rule, which requires that the integral over all frequencies of the real part of the conductivity be independent of the transition, is not satisfied by the conductivities used here. The area under the real part grows as the transition is approached and then drops again below it. (See Figs. 7 and 8.) The easiest way to fix this up would be to have the conductivity ratio versus frequency drop to slightly below 1 and then rise slowly back to 1. Where this happened, the transmission ratios would be greater than 1. (ii) The other possibility is that when the sample is warmed up the detector is also warmed up. This would reduce its sensitivity and thereby reduce the measured normal-state-transmission value. The first of these possibilities is serious, but the other is not, merely requiring a renormalization of the normal-state-transmission data.

The principal object of these experiments has been a measurement of the frequency dependence of the fluctuations, to see if the description given by the time-dependent Ginsburg-Landau equation is applicable. This equation is not on as good a footing as the rest of the Ginsburg-Landau theory. Most of the frequency dependence in the conductivities depends on ω_F, which is twice the relaxation rate in this equation:

$$\omega_F = (16 k_B T/\pi\hbar)\,|T - T_c|/T_c.$$

An attempt was made to fit the measured transmission data for Pb 3 above T_c with ω_F replaced by $1.5\omega_F$ and by $0.6\omega_F$. As shown in Fig. 9, in neither case do the resultant transmission curves agree with the data as well as those calculated using ω_F. The discrepancy is largest at the temperatures closest to T_c. In the upper box, all three curves have been made to coincide at the high-frequency end (as they would do in theory). In the lower box all three have been adjusted to go through the center frequency of the data. This is the fitting method used in Figs. 3–6.

The critical region is defined as

$$\Delta T = \tau_0 R_N^{\square} T_c.$$

In this temperature interval from the transition temperature, at least half of the conductivity is due to fluctuations so that the volume of the fluctuations is large and they should be interacting with each other. The simple theory is expected to break down. However, film Pb 3 has three of the spectra above T_c and two below in this critical region. The calculations agree with the measurements as well within the critical region as without. The same is true of all the other specimens. The reason may well be that within the critical region

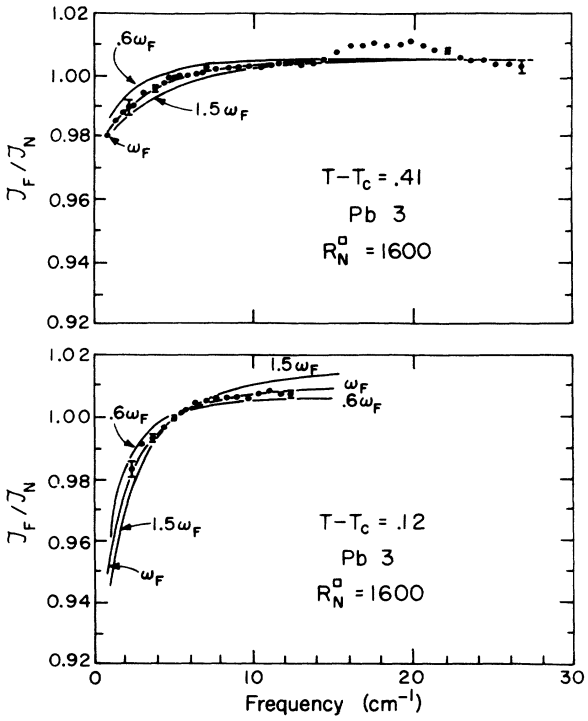

FIG. 9. Effect of changing ω_F on the transmission ratio.

ω_F is very small. ($\omega_F = 0.35$ cm^{-1} at the verge of it in the case of Pb 3.) The measurements are all on the high-frequency tails of the conductivities and these must be unaffected by interactions between the fluctuations. Further, the deviations in the dc resistance from the Aslamazov-Larkin result are often small.

In general, the difference between the experimental data and the theoretical curves is larger below T_c. Again in reference to Pb 3 (Fig. 3), these differences seem to be due to the Mattis-Bardeen conductivities rather than the fluctuation conductivities. The data taken closest to the transition ($T - T_c = -0.007$), where the fluctuations are the largest and the contribution from the quasiparticles the smallest, give the best agreement between experiment and theory. The situation deteriorates as the temperature is reduced away from T_c. To fit the data, the difference between the superconducting and normal-state conductivities needs to be reduced to about 0.6 the values used here.

Figure 10 shows plotted the data and the calculated transmission ratios using the Mattis-Bardeen conductivities alone (dashed line) and the fluctuation conductivities plus the Mattis-Bardeen conductivities (solid line). Two of the spectra for Pb 3 are used. In this figure there has been no fitting of data in any way; the experimental points and theoretical curves are all numerically equal to the values on the figure. Although generally lower than the data, the curve calculated using Schmidt's conductivities gives the shape of the data quite well; that from the Mattis-Bardeen conductivities does not.

The magnitude of the fluctuation effects is quite small, compared to the transmission ratio of the superconducting to state at 4.2 °K to the normal state. For instance, in the case of Pb 6 the maximum distance the transmission ratio in the fluctuation temperature range above T_c ever gets from 1 is 0.96, a 4% variation. The transmission rate for superconducting normal (4.2°/9°) of this same film is 0.75 at 2 cm^{-1}. It rises to 1.27 at 22 cm^{-1} (the energy gap) and then falls off towards 1. It varies 25% on either side of 1. On this scale the transmission ratios near T_c would appear virtually flat.

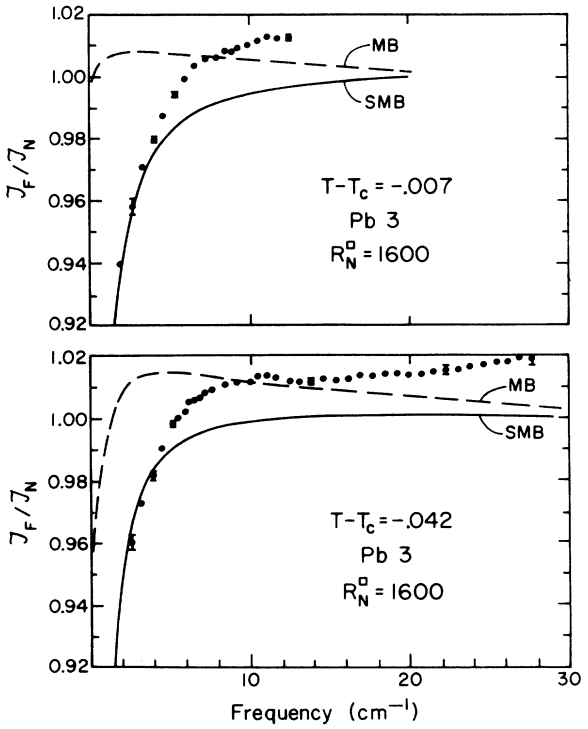

FIG. 10. Transmission ratio vs frequency for two temperatures below T_c for Pb 3. The solid line is from the fluctuation conductivities plus the Mattis-Bardeen conductivities (SMB); the dashed line the MB conductivities alone.

VI. SUMMARY AND CONCLUSIONS

Measurements of the transmission of far-infrared radiation through four thin lead films as a function of temperature were made. The dc resistance of the films was also measured. Both types of measurements showed an increase in the conductivity near T_c.

The experimental data are well described by the conductivities calculated from the Ginsburg-Landau theory. The relaxation rate in the time-dependent equation

$$\omega_F = (16 k_B T/\pi\hbar)[(T - T_c)/T_c]$$

is that which best fits the results of the measurements.

ACKNOWLEDGMENTS

It gives me great pleasure to acknowledge the guidance of Professor A. J. Sievers during this work. His constant interest and enthusiasm, valuable advice, and large measure of practical help were essential to its completion. I have also had many helpful discussions with Professor J. W. Wilkins and Dr. B. R. Patton. Finally, I would like to thank A. Turco for doing a great amount of machining and W. Bement for general technical assistance.

*Work supported by the U. S. Atomic Energy Commission under Contract No. AT(11-1)-3151, Technical Report No. C00-3151-16. Additional support was received from the National Science Foundation under Grant No. GH-33637 through the Cornell Materials Science Center Report No. 1891.

†Present address: Department of Physics, University of Pennsylvania, Philadelphia, Pa. 19174.
[1]R. E. Glover, Phys. Lett. A **25**, 542 (1967).
[2]D. C. Naugle and R. E. Glover, Phys. Lett. A **28**, 110 (1968).
[3]M. Strongin, O. F. Kammerer, J. Crow, R. S. Thompson, and H. L. Fine, Phys. Rev. Lett. **20**, 922 (1968).
[4]W. E. Masker and R. D. Parks, Phys. Rev. B **1**, 2164 (1970).
[5]R. O. Smith, B. Serin, and E. Abrahams, Phys. Lett. A **28**, 224 (1968).
[6]L. R. Testardi, W. A. Reed, P. C. Hohenberg, W. H. Haemmerle, and G. F. Brennert, Phys. Rev. **181**, 800 (1969).
[7]R. S. Thompson, M. Strongin, O. F. Kammerer, and J. E. Crow, Phys. Lett. A **29**, 194 (1969).
[8]L. G. Aslamazov and A. I. Larkin, Phys. Lett. A **26**, 238 (1968); Fiz. Tverd. Tela **10**, 1104 (1968) [Sov. Phys.-Solid State **10**, 875 (1968)].
[9]A. Schmid, Z. Phys. **215**, 210 (1968).
[10]H. Schmidt, Z. Phys. **216**, 336 (1968).
[11]H. Schmidt, Z. Phys. **232**, 442 (1970).
[12]P. B. Miller, Phys. Rev. **118**, 928 (1960).
[13]D. C. Mattis and J. Bardeen, Phys. Rev. **111**, 412 (1958).
[14]D. B. Tanner, Ph. D. thesis (Cornell University, 1972) (unpublished).
[15]G. Eilenberger, Z. Phys. 236, 1 (1970).
[16]L. N. Hadley and D. M. Dennison, J. Opt. Soc. Am. **37**, 451 (1947).
[17]R. V. D'Aiello and S. J. Freedman, Phys. Rev. Lett. **22**, 515 (1969).
[18]S. L. Lehoczky and C. V. Briscoe, Phys. Rev. B **4**, 3938 (1971). Preliminary results were reported in Phys. Rev. Lett. **23**, 695 (1969); and Phys. Rev. Lett. 24, 880 (1970).
[19]I. G. Nolt, R. D. Kirby, C. D. Lytle, and A. J. Sievers, Appl. Opt. **8**, 309 (1969).
[20]H. D. Drew and A. J. Sievers, Appl. Opt. **8**, 2067 (1969).
[21]A. M. Kahan, Infrared Phys. 13, 25 (1973); Cornell University, 1971, Materials Science Center Report (unpublished).
[22]M. Strongin, R. S. Thompson, O. F. Kammerer, and J. E. Crow, Phys. Rev. B 1, 1078 (1970).
[23]K. L. Chapra, *Thin Film Phenomena* (McGraw-Hill, New York, 1969), p. 351ff.
[24]E. H. Sondheimer, Adv. Phys. 1, 1 (1952).